Atmos. Chem. Phys. Discuss., 10, 1005–1034, 2010
www.atmos-chem-phys-discuss.net/10/1005/2010/

Atmospheric Chemistry and Physics Discussions

This discussion paper is/has been under review for the journal Atmospheric Chemistry and Physics (ACP). Please refer to the corresponding final paper in ACP if available.

Technical Note: Hygroscopicity distribution concept for measurement data analysis and modeling of aerosol particle hygroscopicity and CCN activity

H. Su[1], D. Rose[1], Y. F. Cheng[2], S. S. Gunthe[1], A. Massling[2], M. Stock[2], A. Wiedensohler[2], M. O. Andreae[1], and U. Pöschl[1]

[1]Max Planck Institute for Chemistry, 55020 Mainz, Germany
[2]Leibniz Institute for Tropospheric Research, 04318 Leipzig, Germany

Received: 8 December 2009 – Accepted: 21 December 2009 – Published: 18 January 2010

Correspondence to: H. Su (h.su@mpic.de)

Published by Copernicus Publications on behalf of the European Geosciences Union.

Abstract

This paper presents a new concept of hygroscopicity distribution for the analysis and modeling of aerosol particle hygroscopicity and Cloud Condensation Nucleus (CCN) activity. The cumulative particle hygroscopicity distribution function $N(\kappa)$ is defined as the number concentration of particles with an effective hygroscopicity parameter, κ, smaller than the distribution argument κ. From Hygroscopicity Tandem Differential Mobility Analyzer (HTDMA) measurement data, $N(\kappa)$ can be directly derived by solving the κ-Köhler model equation. Similarly, measured CCN efficiency spectra (activation curves) can also be converted into $N(\kappa)$, because the CCN measured at a fixed particle diameter and supersaturation (S) can be regarded as those particles with κ larger than a certain threshold value. Unlike studies calculating only one hygroscopicity parameter value from a CCN efficiency spectrum, the concept of $N(\kappa)$ makes use of the information contained in each point of the spectrum. Model aerosols are used to explain the concept, and exemplary applications are shown with HTDMA and CCN field measurement data.

1 Introduction

Aerosol particles serving as Cloud Condensation Nuclei (CCN) play an important role in the cloud formation process (Pruppacher and Klett, 1997). At a given water vapor supersaturation, the activation of CCN into cloud droplets is determined by particle size and composition, according to Köhler theory (Köhler, 1936). Petters and Kreidenweis (2007) proposed a κ-Köhler theory using a simple parameter, κ, as a quantitative measure of aerosol water uptake characteristics and CCN activity. The values of κ can be determined experimentally by fitting Hygroscopicity Tandem Differential Mobility Analyzer (HTDMA) and CCN measurement data.

Size dependence of κ has been found in CCN measurements of atmospheric aerosols (Rose et al., 2008b; Gunthe et al., 2009; Petters et al., 2009a). However,

ACPD
10, 1005–1034, 2010

very few studies reported different hygroscopicity values among particles of the same size. It would be useful to know such differences, and the influence this would have on the cloud formation process. Internally mixed particles have the same chemical composition and hence the same hygroscopicity, so differences in κ among particles of the same size indicate how well they are mixed. If the κ distribution among particles of a given size can be measured, the (hygroscopicity related) particle mixing state can also be derived.

Thus, κ distribution data complement information about aerosol mixing state obtained with other measurement techniques like the Volatility Tandem Differential Mobility Analyzer (VTDMA) (Orsini et al., 1996), the Single-Particle Soot Photometer (SP2) (Schwarz et al., 2006), Scanning and Transmission Electron Microscopes (STEM) and Single Particle Mass Spectrometers (SPMS) (McMurry et al., 1996; Buzorius et al., 2002; Krejci et al., 2004; Murphy et al., 2006).

In this paper, we introduce a concept of particle hygroscopicity distribution and we show how it can be related to hygroscopicity measurements. Model aerosols are used to explain the concept, and exemplary applications are shown with HTDMA and CCN field measurement data.

2 Concept and methods

2.1 Hygroscopicity distribution

Particle size distributions are widely used in atmospheric and aerosol science. Here we introduce a similar concept, namely, particle hygroscopicity distribution. In an aerosol population, the hygroscopicity of each particle can be described by an "effective" hygroscopicity parameter, κ (Petters and Kreidenweis, 2007; Sullivan et al., 2009). Here "effective" means that the parameter accounts not only for the reduction of water activity by the solute but also for surface tension effects (Rose et al., 2008a; Gunthe et al., 2009; Pöschl et al., 2009).

ACPD
10, 1005–1034, 2010

For atmospheric aerosols, the range of κ typically varies from ~0.01 for combustion aerosol particles up to ~1 for sea-salt particles (Andreae and Rosenfeld, 2008; Niedermeier et al., 2008; Petters et al., 2009a). If we assort the particles by κ, a hygroscopicity distribution can be defined and described in analogy to the size distribution of the aerosol population. In the following, we apply the same terminology and formalisms as used by Seinfeld and Pandis (2006).

The cumulative hygroscopicity distribution function $N(\kappa)$ is hence defined as,

$N(\kappa)$ = number of particles per cm^3 having a hygroscopicity parameter smaller than κ

Note that $N(\kappa)$ can be defined for the whole aerosol population, or just for particles of a specific size (bin). In this paper, $N(\kappa)$ generally refers to a certain particle size (dry particle diameter, D_d). For aerosols with size-dependent particle composition, different distributions, $N(\kappa)$, can be expected for different values of D_d.

The concept of the particle hygroscopicity distribution is not limited to the κ parameter. Similar distributions can also be defined and applied with other hygroscopicity parameters, e.g., $N(\rho_{ion})$ for the equivalent ion density as proposed by Rissler et al. (2006) and Wex et al. (2007) or $N(\varepsilon_{AS})$ for the equivalent soluble fraction as used in many earlier studies mostly referring to ammonium sulfate (or bisulfate; Gunthe et al., 2009 and references therein). Moreover, similar formalisms could also be based on the van not Hoff factor i_s (McDonald, 1953) or the product of the stoichiometric dissociation number and osmotic coefficient of the solute $\nu_s\Phi_s$, (Robinson and Stokes, 1959; Rose et al., 2008a) averaged over all chemical components of a particle according to mixing rules (e.g., the Zdanovski-Stokes-Robinson), or more advanced models taking into account complex solute interactions and concentration dependencies (e.g., extended aerosol inorganic model, Clegg et al., 2008). Here we focus on the effective hygroscopicity parameter κ, which can be directly and efficiently linked to field measurement data as detailed below.

The normalized cumulative hygroscopicity distribution function $N^*(\kappa)$ is defined by the following equation, where N_t is the total aerosol particle number concentration at

ACPD
10, 1005–1034, 2010

the size bin in which $N^*(\kappa)$ is defined. After normalization, the maximum value of $N^*(\kappa)$ equals one.

$$N^*(\kappa) = \frac{N(\kappa)}{N_t} \text{ in which } N_t = N(\infty) \quad (1)$$

Aerosol hygroscopicity parameters determined from HTDMA and CCN measurements are often presented in discrete forms (tables or graphs), which are difficult to generalize and use in theoretical studies. Thus, we pursued the idea of using simple mathematical functions to represent measured distributions. In atmospheric aerosol science, lognormal distributions (Aitchison and Brown, 1957) often provide a good fit to observed data and are commonly used (Seinfeld and Pandis, 2006).

For an aerosol population with lognormally distributed hygroscopicity, κ, the normalized cumulative hygroscopicity distribution function is given by

$$N^*(\kappa) = \frac{1}{2} + \frac{1}{2}\text{erf}\left(\frac{\log\kappa - \log\overline{\kappa}}{\sqrt{2}\log\sigma_{g,\kappa}}\right) \quad (2)$$

where erf is the Gauss error function, and $\overline{\kappa}$ and $\sigma_{g,\kappa}$ are the two parameters describing the distribution. The parameter $\overline{\kappa}$ is the geometric mean value of κ. The parameter $\sigma_{g,\kappa}$ is the geometric standard deviation. For a homogeneously mixed, i.e., fully internally mixed aerosol population, $\sigma_{g,\kappa}$=1. Increasing values of $\sigma_{g,\kappa}$ indicate increasing heterogeneity (external mixing) of the aerosol population.

The normalized hygroscopicity distribution function $n^*(\kappa)$ can be calculated from the normalized cumulative hygroscopicity distribution function as follows:

$$n^*(\kappa) = \frac{dN^*(\kappa)}{d\log\kappa} \quad (3)$$

Note that unlike $N^*(\kappa)$, $n^*(\kappa)$ is not limited to a maximum value of one.

ACPD
10, 1005–1034, 2010

2.2 HTDMA data analysis

In HTDMA measurements, a nearly mono-disperse dry particle fraction of the size D_d is selected by the first Differential Mobility Analyzer (DMA) and afterwards equilibrated to a defined Relative Humidity (RH). Then a second DMA is used to measure the size distribution of the equilibrated wet particles, $n(D_w)$ and to calculate the cumulative wet particle size distribution function, $N(D_w)$. According to κ-Köhler theory (Eq. 4; Petters and Kreidenweis, 2007), the equilibrium wet particle size, D_w, depends on particle hygroscopicity (κ) and on RH, or the water vapor saturation ratio, respectively (s=RH/100%).

$$s = \frac{D_w^3 - D_d^3}{D_w^3 - D_d^3(1-\kappa)} \exp\left(\frac{4\sigma_{sol} M_w}{RT\rho_w D_w}\right) \quad (4)$$

Here σ_{sol} is the surface tension of a solution droplet (wet particle), M_w is the molar mass of water, R is the universal gas constant, T is the temperature and ρ_w is the density of pure water. Assuming that σ_{sol} equals the surface tension of water (σ_w=0.072 J m^{-2} at 298.15 K), wet particle diameters can be directly converted into effective hygroscopicity parameters:

$$\kappa = 1 - \frac{D_w^3}{D_d^3} + \frac{D_w^3 - D_d^3}{sD_d^3} \exp\left(\frac{4\sigma_w M_w}{RT\rho_w D_w}\right) \quad (5)$$

By applying Eq. (5), the normalized cumulative wet particle size distribution function $N^*(D_w)$ can be converted into $N^*(\kappa)$. Figure 1 shows an exemplary case of $N^*(\kappa)$ derived from HTDMA measurements in Beijing, China (Massling et al., 2009). The exemplary case in Fig. 1 is based on one-day average HTDMA measurement results from Beijing, on 12 June 2004. The dry particle diameters selected by the first DMA were 80 nm and 150 nm, respectively. Further details about the measurement campaign, instrumentation and experimental conditions are given by Massling et al. (2009). The

ACPD
10, 1005–1034, 2010

lower end of the exemplary distribution curves in Fig. 1 reflects the first HTDMA size channel larger than the nominally selected diameter, indicating that 10–20% of the mono-disperse particles have even smaller κ values close to zero. These particles are most likely externally mixed soot particles freshly emitted from strong local sources (e.g., Garland et al., 2008; Rose et al., 2008b; Cheng et al., 2009; Garland et al., 2009; Massling et al., 2009; Wehner et al., 2009). The steep increase around kappa ~0.5 indicates a lognormal mode of particles, which consists likely of varying amounts of sulfate, organics and aged soot (Massling et al., 2009; Wiedensohler et al., 2009).

Equation (5) has already been used in earlier HTDMA studies (Petters and Kreidenweis, 2007; Petters et al., 2009b; Wex et al., 2009), and its application for deriving hygroscopicity distributions will not be discussed any further in this paper. HTDMA data can easily be further analyzed and plotted as illustrated below for CCN data (Sects. 3 and 4).

2.3 CCN data analysis

The size-resolved CCN measurement usually provides two size-dependent parameters, N_{CN} and N_{CCN}. The parameter N_{CN} is the total number concentration in one size bin. The parameter N_{CCN} is the number concentration of particles activated at a given water vapor supersaturation, S, and according to κ-Köhler theory, particles activated at S have a hygroscopicity parameter κ larger than a critical value κ_{cri}:

$$N_{CCN} = \int_{\kappa_{cri}}^{\infty} n(\kappa) d \log \kappa = N_{CN} - \int_{0}^{\kappa_{cri}} n(\kappa) d \log \kappa = N_{CN} - N(\kappa_{cri}) \quad (6)$$

$$\kappa_{cri} = f(S, D_d) \approx \frac{4A^3}{27(\ln(S/100\% + 1))^2 D_d^3}, \text{ with } A = \frac{\sigma_{sol} M_w}{RT\rho_w} \text{ and } \sigma_{sol} = \sigma_w \quad (7)$$

Note that the critical value of the effective hygroscopicity parameter (κ_{cri}) is defined in analogy to the other critical parameters of CCN activation, i.e., the "critical" size of dry

ACPD
10, 1005–1034, 2010

particles ($D_{d,cri}$) and the "critical" supersaturation (S_{cri}) above which particles will be activated:

$$D_{d,cri} \approx \sqrt[3]{\frac{4A^3}{27\kappa(\ln(S/100\%+1))^2}} \quad (8)$$

$$S_{cri} \approx 100\% * \left(\exp\left(\sqrt{\frac{4A^3}{27\kappa D_d^3}} \right) - 1 \right) \quad (9)$$

Since $N(\kappa_{cri})$ means the number concentration of particles with hygroscopicity smaller than κ_{cri}, the sum of $N(\kappa_{cri})$ and N_{CCN} equals N_{CN}. Equations (10) and (11) show the expression of $N(\kappa_{cri})$ and its normalized form $N^*(\kappa_{cri})$ by CCN measurement results.

$$N(\kappa_{cri}) = N_{CN} - N_{CCN} \quad (10)$$

$$N^*(\kappa_{cri}) = 1 - N_{CCN}/N_{CN} \quad (11)$$

According to κ-Köhler theory, κ_{cri} depends on the size of particles and the supersaturation, S, as described by Eq. (7). For CCN measurements at a fixed dry particle size D_d, a given value of S corresponds to a specific value of κ_{cri} (as in Eq. 7) and the measured values of N_{CCN} and N_{CN} yield a value of $N^*(\kappa_{cri})$ (as in Eq. 11). To obtain the complete distribution function $N(\kappa)$ for a given particle size D_d, S can be varied so that κ_{cri} covers the whole relevant range of κ. By applying the same procedure for particles at other D_d, the complete representation of $N^*(\kappa)$ in the $D_d-\kappa$ plane can be obtained. This approach (called method I or "S scan"), of first keeping D_d constant and varying S, then choosing another D_d and doing the same procedure, has been adopted in several studies (e.g., Dusek et al., 2006; Frank et al., 2006). Alternatively, S can be kept constant while varying D_d. Then another S is selected and the same procedure is applied (called method II or "D_d scan", e.g., Rose et al., 2008a; Gunthe et al., 2009; Petters et al., 2009a). This method yields one value of $N^*(\kappa_{cri})$ for each value of D_d investigated at a constant S.

Figure 2 illustrates the two different methods used in measuring $N^*(\kappa)$ where each line represents one measurement cycle. Method I is shown by the vertical dashed lines (constant D_d). Method II is represented by the tilted solid lines (constant S).

In principle, method I and II are mathematically equivalent with regard to probing the surface of the $N^*(\kappa)$ distributions in the D_d–κ plane. Method I is easier to interpret and understand, but because most of the recently reported CCN measurement studies have applied method II, our subsequent discussions will be focused on method II (size-resolved CCN measurements, varying D_d at a constant S). As mentioned above, $N(\kappa)$ can be defined for the whole aerosol population, or just for particles of a specific size (bin). However, only size-resolved CCN measurement data can be used to determine $N(\kappa)$, because of the dependence of κ_{cri} on D_d. Therefore $N(\kappa)$ derived from size-resolved CCN measurements always refers to a specific D_d.

2.4 Uncertainties

The uncertainty of $N^*(\kappa)$ derived from size-resolved CCN measurements is determined by the uncertainty of the N_{CCN}/N_{CN} measurement data, which depends on various factors like instrument calibration, counting statistics, and various correction factors (counting efficiency, electric charge, DMA transfer function, particle shape, etc.; (Rose et al., 2008a). Moreover, κ values determined by HTDMA measurement can be different from κ values determined by CCN measurements (Petters and Kreidenweis, 2007), because of the general dependence of κ, i_s and Φ_s on solute concentrations (Mikhailov et al., 2004; Rose et al., 2008a; Reutter et al., 2009) and potential solubility effects (Petters and Kreidenweis, 2008). Thus, the uncertainty, applicability, and extrapolation of hygroscopicity distributions determined by HTDMA or CCN measurements depend on the ambient and experimental conditions and on the quality of the measurement data (e.g., Rissler et al., 2006; Svenningson et al., 2006; Vestin et al., 2007; Gunthe et al., 2009; Petters et al., 2009a; Wex et al., 2009). If the chemical composition and properties of a particle population are known or can be estimated, it would be possible to calculate hygroscopicity distributions as a function of relative

ACPD
10, 1005–1034, 2010

humidity. As indicated above, simple mixing rules or advanced models could be used for such purposes, and surface tension effects could also be taken into account. A detailed discussion of such aspects, however, would go beyond the scope of the present manuscript, which is aimed at introducing and illustrating the basic concept.

3 CCN efficiency spectra calculated from model hygroscopicity distributions

The concept of $N(\kappa)$ helps in interpreting the CCN measurement data. Previous studies tended to calculate a single κ value from one CCN efficiency spectrum, e.g., only the κ_{cri} corresponding to the diameter D_d where 50% of the particles are activated. In fact, each N_{CCN}/N_{CN} at size D_d represents one $N^*(\kappa)$ value at κ_{cri} corresponding to D_d. In this section, we show how $N^*(\kappa)$ are reflected in the CCN efficiency spectra (activation curves) of size-resolved CCN measurements. Three distributions of $N^*(\kappa)$ (in Table 1) and the corresponding activation curves by D_d scans (method II) are presented.

3.1 Internally mixed aerosols

In Case A, the aerosol is assumed to be 100% internally mixed. All particles have the same composition and hygroscopicity corresponding to a mono-disperse distribution $N^*(\kappa)$ with $\sigma_{g,\kappa}$=1 and $\overline{\kappa}$=0.2. If we made a CCN measurement of this aerosol at S=0.86%, 0.26% and 0.067%, the ideally obtained CCN efficiency spectra would be perfect step functions as shown in Fig. 3. All particles are activated at $D_d \geq D_{d,cri}$ and none are activated at $D_d < D_{d,cri}$ ($D_{d,cri}$ can be calculated by Eq. 8). Note that such step functions could be observed only under assumed ideal measurement conditions. In practice, experimental uncertainties will result in some dispersion even for pure calibration aerosols (Rose et al., 2008a).

ACPD
10, 1005–1034, 2010

3.2 Simple externally mixed aerosols (single-mode lognormal κ distribution)

In Case B, we assume an aerosol with a size-independent κ distribution consisting of a single lognormal mode, i.e., $N^*(\kappa)=\frac{1}{2}+\frac{1}{2}\mathrm{erf}\left(\frac{\log\kappa-\log\overline{\kappa}}{\sqrt{2}\log\sigma_{g,\kappa}}\right)$. The values of $\overline{\kappa}$ and $\sigma_{g,\kappa}$ were set to 0.2 and 1.583, respectively, and these values are the same over all D_d. Figure 4 shows the $n^*(\kappa)$ of Case B aerosols. If we made CCN measurements of such aerosol at S=0.86%, 0.26% and 0.067% (tilted lines in Fig. 4), the obtained CCN efficiency spectra would be cumulative lognormal distribution functions as shown in Fig. 3. Similar CCN efficiency spectra have been observed for well-mixed and aged atmospheric aerosols in several field measurements (Rose et al., 2008b).

3.3 Complex externally mixed aerosols (two-mode lognormal κ distribution)

In Case C, we assumed an aerosol with two lognormally distributed modes of $N^*(\kappa)$. In one mode (mode 1), κ is size-independent with $\overline{\kappa_1}$=0.05 and $\sigma_{g,\kappa,1}$=1.1. In the other mode (mode 2), κ is size-dependent with $\overline{\kappa_2(D_\mathrm{d})}=0.2(D_\mathrm{d}/20\ \mathrm{nm})^{0.4}$ and $\sigma_{g,\kappa,2}$=1.587, as illustrated in Fig. 5. If we made a CCN measurement of this aerosol at S=0.86%, 0.26% and 0.067% (tilted lines in Fig. 5), the obtained CCN efficiency spectra would show the existence of the two modes as illustrated in Fig. 3. Despite knowing the size dependence of κ in mode 2, one cannot easily see it from the CCN efficiency spectra in Fig. 3. That is one of the reasons that we recommend using retrieved $N^*(\kappa)$ as an analysis tool.

3.4 Retrieval of $N^*(\kappa)$ from CCN efficiency spectra

To obtain $N^*(\kappa)$ from an observed CCN efficiency spectrum (activation curve, by D_d scan), each data pair of $N_\mathrm{CCN}/N_\mathrm{CN}$ vs. D_d in the CCN efficiency spectrum is converted into a corresponding data pair of $N^*(\kappa_\mathrm{cri})$ vs. κ_cri by Eqs. (11) and (7). The $N^*(\kappa)$ obtained from the CCN efficiency spectra in Fig. 3 are shown in Fig. 6.

ACPD
10, 1005–1034, 2010

Compared with the CCN efficiency spectra, the form of $N^*(\kappa)$ distributions presents the particle hygroscopic properties more explicitly. Both the shape and size dependence of particle $N^*(\kappa)$ can be seen from Fig. 6. In Case A and Case B, the $N^*(\kappa)$ calculated from CCN efficiency spectra are consistent with our assumptions, showing a lognormal distribution of $\overline{\kappa}$=0.2 and $\sigma_{g,\kappa}$=1 or 1.587, respectively. In Case C, the two-mode lognormal distributions are clearly seen. The first mode has a $\overline{\kappa_1}$=0.05 and the second mode shows an increasing trend in $\overline{\kappa_2}$ for measurements at increasing D_d (because in CCN measurements a lower S corresponds to larger D_d for the same κ_{cri}).

4 Hygroscopicity distributions calculated from measured CCN efficiency spectra

In the CAREBEIJING 2006 campaign size-resolved CCN measurements at different S were carried out from 12 August to 8 September (Garland et al., 2009; Wiedensohler et al., 2009). The CCN data were recorded and processed in the same way as described in detail by Rose et al. (2008b) and Gunthe et al. (2009).

Figure 7 shows the measured CCN efficiency spectra averaged over the campaign, and Fig. 8 shows the corresponding distributions $N^*(\kappa)$, which are comparable to the ones obtained for the model aerosol Case C (Fig. 5). Over 95% of the ~1536 individual distributions $N^*(\kappa)$ recorded during the campaign can be fitted by cumulative lognormal distribution functions with coefficients of determination R^2>0.8, supporting the idea that lognormal distribution functions are well suited not only for describing the size distribution but also the hygrocopicity distribution of atmospheric particles.

Figure 9 shows the measurement-derived values of $n^*(\kappa)$, i.e. the derivative of $N^*(\kappa)$, interpolated as a function of κ and D_d (analogous to Figs. 4 and 5). The boundaries of the contour plot are constrained by the second last point on each end of the measured CCN spectra, because the derivative is not well defined for the last point. The contour plot exhibits a pronounced mode around κ~0.2–0.6, whereby κ tends to increase with D_d in analogy Fig. 5 (model aerosol Case C).

Similar size dependencies of κ have also been observed in recent field studies of atmospheric aerosols (Rose et al., 2008b; Gunthe et al., 2009) and chamber experiments with combustion aerosols (Petters et al., 2009a). As illustrated in Fig. 8, the measurement data indicate a significant particle fraction (~10%) with κ values <0.1. These are most likely externally mixed soot particles freshly emitted from strong local and regional sources (Garland et al., 2008; Rose et al., 2008b; Cheng et al., 2009; Garland et al., 2009; Wehner et al., 2009). They would likely show up as a low hygroscopicity mode at the bottom of Fig. 9 (in analogy to Fig. 5) if the available data would cover this area. The CCN measurement data available for Beijing, however, provide only an upper limit value for the effective hygroscopicity parameter of these particles and do not allow a full characterization of the low hygroscopicity mode (insufficient data at high S and high D_d, respectively).

5 Conclusions

In this study, the concept of a particle hygroscopicity distribution has been introduced and related to HTDMA and size-resolved CCN measurements. Model aerosols were used to illustrate the concept, and its applicability has been demonstrated with field measurement data of polluted megacity air in Beijing exhibiting a lognormally distributed mode with κ values around 0.2–0.4, and a significant particle fraction (ca. 10–20%) with κ values <0.1, which can be attributed to externally mixed soot particles (Garland et al., 2008; Rose et al., 2008b; Cheng et al., 2009; Garland et al., 2009; Massling et al., 2009; Wehner et al., 2009). For full and refined coverage of the effective hygroscopicity distribution of aerosol particles as relevant for CCN activation, we recommend higher resolution and larger ranges of S and D_d for future size-resolved CCN measurements in regions where a low hygroscopicity mode can be expected and observed (e.g., in regions with strong sources of pyrogenic particles from biomass burning and fuel combustion). The hygroscopicity distribution concept may also extend the usefulness of HTDMA and CCN counters for the characterization of aerosol mixing

ACPD
10, 1005–1034, 2010

state in field and laboratory studies. With the help of single particle analysis techniques, it should become possible to predict aerosol hygroscopicity distributions from chemical composition data. Accordingly, we propose and intend to use hygroscopicity distributions for testing the influence of observed and predicted aerosol mixing state on the formation of cloud droplets in atmospheric model studies.

Acknowledgements. This work was funded by the Max Planck Society (MPG) and the European integrated project on aerosol cloud climate and air quality interactions (No 036833-2, EUCAARI). The authors gratefully acknowledge support by the CAREBEIJING2006 group. The authors would also like to thank T. W. Andreae and D. Pickersgill for their help in text editing.

The service charges for this open access publication
have been covered by the Max Planck Society.

References

Aitchison, J. and Brown, J. A. C.: The lognormal distribution function, Cambridge Univ. Press, Cambridge, UK, 1957.

Andreae, M. O. and Rosenfeld, D.: Aerosol-cloud-precipitation interactions. Part 1. The nature and sources of cloud-active aerosols, Earth-Sci. Rev., 89, 13–41, 2008.

Buzorius, G., Zelenyuk, A., Brechtel, F., and Imre, D.: Simultaneous determination of individual ambient particle size, hygroscopicity and composition, Geophys. Res. Lett., 29(20), doi:10.1029/2001gl014221, 2002.

Cheng, Y. F., Berghof, M., Garland, R. M., Wiedensohler, A., Wehner, B., Müller, T., Su, H., Zhang, Y. H., Achtert, P., Nowak, A., Pöschl, U., Zhu, T., Hu, M., and Zeng, L. M.: Influence of soot mixing state on aerosol light absorption and single scattering albedo during air mass aging at a polluted regional site in northeastern china, J. Geophys. Res., 114, D00G10, doi:10.1029/2008jd010883, 2009.

Clegg, S. L., Kleeman, M. J., Griffin, R. J., and Seinfeld, J. H.: Effects of uncertainties in the thermodynamic properties of aerosol components in an air quality model - Part 1: Treatment of inorganic electrolytes and organic compounds in the condensed phase, Atmos. Chem. Phys., 8, 1057–1085, 2008, http://www.atmos-chem-phys.net/8/1057/2008/.

Dusek, U., Frank, G. P., Hildebrandt, L., Curtius, J., Schneider, J., Walter, S., Chand, D., Drewnick, F., Hings, S., Jung, D., Borrmann, S., and Andreae, M. O.: Size matters more than chemistry for cloud-nucleating ability of aerosol particles, Science, 312, 1375–1378, doi:10.1126/science.1125261, 2006.

Frank, G. P., Dusek, U., and Andreae, M. O.: Technical note: A method for measuring size-resolved CCN in the atmosphere, Atmos. Chem. Phys. Discuss., 6, 4879–4895, 2006,

Garland, R. M., Yang, H., Schmid, O., Rose, D., Nowak, A., Achtert, P., Wiedensohler, A., Takegawa, N., Kita, K., Miyazaki, Y., Kondo, Y., Hu, M., Shao, M., Zeng, L. M., Zhang, Y. H., Andreae, M. O., and Pöschl, U.: Aerosol optical properties in a rural environment near the mega-city Guangzhou, China: implications for regional air pollution, radiative forcing and remote sensing, Atmos. Chem. Phys., 8, 5161–5186, 2008, http://www.atmos-chem-phys.net/8/5161/2008/.

Garland, R. M., Schmid, O., Nowak, A., Achtert, P., Wiedensohler, A., Gunthe, S. S., Takegawa, N., Kita, K., Kondo, Y., Hu, M., Shao, M., Zeng, L. M., Zhu, T., Andreae, M. O., and Pöschl, U.: Aerosol optical properties observed during campaign of air quality research in Beijing 2006 (carebeijing-2006): characteristic differences between the inflow and outflow of Beijing city air, J. Geophys. Res., 114, D00G04, doi:10.1029/2008jd010780, 2009.

Gunthe, S. S., King, S. M., Rose, D., Chen, Q., Roldin, P., Farmer, D. K., Jimenez, J. L., Artaxo, P., Andreae, M. O., Martin, S. T., and Pöschl, U.: Cloud condensation nuclei in pristine tropical rainforest air of Amazonia: size-resolved measurements and modeling of atmospheric aerosol composition and CCN activity, Atmos. Chem. Phys., 9, 7551–7575, 2009, http://www.atmos-chem-phys.net/9/7551/2009/.

Köhler, H.: The nucleus in the growth of hygroscopic droplets, T. Faraday Soc., 32, 1152–1161, 1936.

Krejci, R., Ström, J., de Reus, M., and Sahle, W.: Single particle analysis of the accumulation mode aerosol over the northeast Amazonian tropical rain forest, Surinam, South America, Atmos. Chem. Phys., 5, 3331–3344, 2005, http://www.atmos-chem-phys.net/5/3331/2005/.

Massling, A., Stock, M., Wehner, B., Wu, Z. J., Hu, M., Brügemann, E., Gnauk, T., Herrmann, H., and Wiedensohler, A.: Size segregated water uptake of the urban submicrometer aerosol in Beijing, Atmos. Environ., 43, 1578–1589, 2009.

McDonald, J. E.: Erroneous cloud-physics applications of raoult law, J. Meteorol., 10, 68–78, 1953.

McMurry, P. H., Litchy, M., Huang, P.-F., Cai, X., Turpin, B. J., Dick, W. D., and Hanson, A.: Elemental composition and morphology of individual particles separated by size and hygroscopicity with the tdma, Atmos. Environ., 30, 101–108, 1996.

Mikhailov, E., Vlasenko, S., Niessner, R., and Pöschl, U.: Interaction of aerosol particles composed of protein and saltswith water vapor: hygroscopic growth and microstructural rearrangement, Atmos. Chem. Phys., 4, 323–350, 2004, http://www.atmos-chem-phys.net/4/323/2004/.

Murphy, D. M., Cziczo, D. J., Froyd, K. D., Hudson, P. K., Matthew, B. M., Middlebrook, A. M., Peltier, R. E., Sullivan, A., Thomson, D. S., and Weber, R. J.: Single-particle mass spectrometry of tropospheric aerosol particles, J. Geophys. Res., 111, D23S32, doi:10.1029/2006jd007340, 2006.

Niedermeier, D., Wex, H., Voigtländer, J., Stratmann, F., Brüggemann, E., Kiselev, A., Henk, H., and Heintzenberg, J.: LACIS-measurements and parameterization of sea-salt particle hygroscopic growth and activation, Atmos. Chem. Phys., 8, 579–590, 2008, http://www.atmos-chem-phys.net/8/579/2008/.

Orsini, D. A., Wiedensohler, A., and Covert, D. S.: Volatility measurements of atmospheric aerosols in the mid and south pacific using a volatility-tandem-differential-mobility-analyzer, J. Aerosol Sci., 27, S53–S54, 1996.

Pöschl, U., Rose, D., and Andreae, M. O.: Climatologies of cloudrelated aerosols – part 2: Particle hygroscopicity and cloud condensation nuclei activity, in: Clouds in the perturbed climate system, edited by: Heintzenberg, J. and Charlson, R. J., MIT Press, Cambridge, 2009.

Petters, M. D. and Kreidenweis, S. M.: A single parameter representation of hygroscopic growth and cloud condensation nucleus activity, Atmos. Chem. Phys., 7, 1961–1971, 2007, http://www.atmos-chem-phys.net/7/1961/2007/.

Petters, M. D., Carrico, C. M., Kreidenweis, S. M., Prenni, A. J., DeMott, P. J., Collett, J. L., Jr., and Moosmüller, H.: Cloud condensation nucleation activity of biomass burning aerosol, J. Geophys. Res., 114, D22205, doi:10.1029/2009jd012353, 2009a.

Petters, M. D., Wex, H., Carrico, C. M., Hallbauer, E., Massling, A., McMeeking, G. R., Poulain, L., Wu, Z., Kreidenweis, S. M., and Stratmann, F.: Towards closing the gap between hygroscopic growth and activation for secondary organic aerosol - Part 2: Theoretical approaches, Atmos. Chem. Phys., 9, 3999–4009, 2009, http://www.atmos-chem-phys.net/9/3999/2009/.

Pruppacher, H. R. and Klett, J. D.: Microphysics of clouds and precipitation, Kluwer Academic Publishers, Dordrecht, 1997.

Reutter, P., Su, H., Trentmann, J., Simmel, M., Rose, D., Gunthe, S. S., Wernli, H., Andreae, M. O., and Pöschl, U.: Aerosol- and updraft-limited regimes of cloud droplet formation: influence of particle number, size and hygroscopicity on the activation of cloud condensation nuclei (CCN), Atmos. Chem. Phys., 9, 7067–7080, 2009, http://www.atmos-chem-phys.net/9/7067/2009/.

Rissler, J., Vestin, A., Swietlicki, E., Fisch, G., Zhou, J., Artaxo, P., and Andreae, M. O.: Size distribution and hygroscopic properties of aerosol particles from dry-season biomass burning in Amazonia, Atmos. Chem. Phys., 6, 471–491, 2006, http://www.atmos-chem-phys.net/6/471/2006/.

Robinson, R. A. and Stokes, R. H.: Electrolyte solutions, revised, Butterworths Scientific Pub, London, 1959.

Rose, D., Gunthe, S. S., Mikhailov, E., Frank, G. P., Dusek, U., Andreae, M. O., and Pöschl, U.: Calibration and measurement uncertainties of a continuous-flow cloud condensation nuclei counter (DMT-CCNC): CCN activation of ammonium sulfate and sodium chloride aerosol particles in theory and experiment, Atmos. Chem. Phys., 8, 1153–1179, 2008a, http://www.atmos-chem-phys.net/8/1153/2008/.

Rose, D., Nowak, A., Achtert, P., Wiedensohler, A., Hu, M., Shao, M., Zhang, Y., Andreae, M. O., and Pöschl, U.: Cloud condensation nuclei in polluted air and biomass burning smoke near the mega-city Guangzhou, China - Part 1: Size-resolved measurements and implications for the modeling of aerosol particle hygroscopicity and CCN activity, Atmos. Chem. Phys. Discuss., 8, 17343–17392, 2008b, http://www.atmos-chem-phys-discuss.net/8/17343/2008/.

Schwarz, J. P., Gao, R. S., Fahey, D. W., Thomson, D. S., Watts, L. A., Wilson, J. C., Reeves, J. M., Darbeheshti, M., Baumgardner, D. G., Kok, G. L., Chung, S. H., Schulz, M., Hendricks, J., Lauer, A., Kärcher, B., Slowik, J. G., Rosenlof, K. H., Thompson, T. L., Langford, A. O., Loewenstein, M., and Aikin, K. C.: Single-particle measurements of midlatitude black carbon and light-scattering aerosols from the boundary layer to the lower stratosphere, J. Geophys. Res., 111, D16207, doi:10.1029/2006jd007076, 2006.

Seinfeld, J. H. and Pandis, S. N.: Atmospheric chemistry and physics, from air pollution to climate change, John Wiley, New York, 362 p., 2006.

Sullivan, R. C., Moore, M. J. K., Petters, M. D., Kreidenweis, S. M., Roberts, G. C., and Prather, K. A.: Effect of chemical mixing state on the hygroscopicity and cloud nucleation properties of calcium mineral dust particles, Atmos. Chem. Phys., 9, 3303–3316, 2009, http://www.atmos-chem-phys.net/9/3303/2009/.

Svenningsson, B., Rissler, J., Swietlicki, E., Mircea, M., Bilde, M., Facchini, M. C., Decesari, S., Fuzzi, S., Zhou, J., Mønster, J., and Rosenørn, T.: Hygroscopic growth and critical supersaturations for mixed aerosol particles of inorganic and organic compounds of atmospheric relevance, Atmos. Chem. Phys., 6, 1937–1952, 2006, http://www.atmos-chem-phys.net/6/1937/2006/.

Vestin, A., Rissler, J., Swietlicki, E., Frank, G. P., and Andreae, M. O.: Cloud-nucleating properties of the amazonian biomass burning aerosol: Cloud condensation nuclei measurements and modeling, J. Geophys. Res., 112, D14201, doi:10.1029/2006jd008104, 2007.

Wehner, B., Berghof, M., Cheng, Y. F., Achtert, P., Birmili, W., Nowak, A., Wiedensohler, A., Garland, R. M., Pöschl, U., Hu, M., and Zhu, T.: Mixing state of nonvolatile aerosol particle fractions and comparison with light absorption in the polluted Beijing region, J. Geophys. Res., 114, D00G17, doi:10.1029/2008jd010923, 2009.

Wex, H., Hennig, T., Salma, I., Ocskay, R., Kiselev, A., Henning, S., Massling, A., Wiedensohler, A., and Stratmann, F.: Hygroscopic growth and measured and modeled critical super-saturations of an atmospheric hulis sample, Geophys. Res. Lett., 34, L02818, doi:10.1029/2006gl028260, 2007.

Wex, H., Petters, M. D., Carrico, C. M., Hallbauer, E., Massling, A., McMeeking, G. R., Poulain, L., Wu, Z., Kreidenweis, S. M., and Stratmann, F.: Towards closing the gap between hygroscopic growth and activation for secondary organic aerosol: Part 1 - Evidence from measurements, Atmos. Chem. Phys., 9, 3987–3997, 2009, http://www.atmos-chem-phys.net/9/3987/2009/.

Wiedensohler, A., Cheng, Y. F., Nowak, A., Wehner, B., Achtert, P., Berghof, M., Birmili, W., Wu, Z. J., Hu, M., Zhu, T., Takegawa, N., Kita, K., Kondo, Y., Lou, S. R., Hofzumahaus, A., Holland, F., Wahner, A., Gunthe, S. S., Rose, D., Su, H., and Pöschl, U.: Rapid aerosol particle growth and increase of cloud condensation nucleus activity by secondary aerosol formation and condensation: A case study for regional air pollution in Northeastern China, J. Geophys. Res., 114, D00G08, doi:10.1029/2008jd010884, 2009.

Table 1. Normalized cumulative hygroscopicity (κ) distribution function for exemplary aerosols (Case A, Case B, Case C).

Normalized Cumulative	$N^*(\kappa)=\frac{1}{2}+\frac{a}{2}\mathrm{erf}\left(\frac{\log\kappa-\log\overline{\kappa_1}}{\sqrt{2}\log\sigma_{g,\kappa,1}}\right)+\frac{1-a}{2}\mathrm{erf}\left(\frac{\log\kappa-\log\overline{\kappa_2}}{\sqrt{2}\log\sigma_{g,\kappa,2}}\right)$				
Hygroscopicity (κ) Distribution Function	a	$\overline{\kappa_1}$	$\sigma_{g,\kappa,1}$	$\overline{\kappa_2}$	$\sigma_{g,\kappa,2}$
Case A	1	0.2	1	–	–
Case B	1	0.2	1.587	–	–
Case C	0.2	0.05	1.1	$\overline{\kappa_2(D_d)}=0.2(D_\mathrm{d}/20\ \mathrm{nm})^{0.4}$	1.587

The parameter a represents the relative proportion of particles in mode 1. The erf function is the Gauss error function.

ACPD
10, 1005–1034, 2010

Table 2. Notation (frequently used symbols).

Symbol	Unit	Quantity
D_d	m (unless specified)	Dry particle diameter
$D_{d,cri}$	m (unless specified)	Critical dry particle diameter
M_w	kg mol^{-1}	Molar mass of water
N_{CCN}	cm^{-3}	The number concentration of CCN particles in one size bin
N_{CN}	cm^{-3}	The total particle number concentration in one size bin
$N(D_w)$	cm^{-3}	Cumulative wet particle size distribution
$N^*(D_w)$		Normalized cumulative wet particle size distribution
N_t	cm^{-3}	Total aerosol number concentration
$N(\kappa)$	cm^{-3}	Cumulative particle hygroscopicity distribution, defined as the number concentration of particles with a hygroscopicity parameter smaller than a certain value κ ($N(\kappa)$ refers to a single size bin)
$N^*(\kappa)$		Normalized cumulative particle hygroscopicity distribution ($N^*(\kappa)$ refers to a single size bin)
$n(D_w)$	cm^{-3}	Wet particle size distribution
$n^*(\kappa)$		Normalized particle hygroscopicity distribution ($n^*(\kappa)$ refers to a single size bin)
R	J K^{-1} mol^{-1}	Universal gas constant
S	%	Water vapor supersaturation
S_{cri}	%	Critical water vapor supersaturation
s		Water vapor saturation ratio
T	K	Temperature
κ		Effective hygroscopicity parameter
κ_{cri}		Critical effective hygroscopicity parameter
$\sigma_{g,\kappa}$		Geometric standard deviation in a lognormal κ distribution
σ_{sol}	J m^{-2}	Surface tension of solution droplet
σ_w	J m^{-2}	Surface tension of pure water
ρ_w	kg m^{-3}	Density of pure water

ACPD
10, 1005–1034, 2010

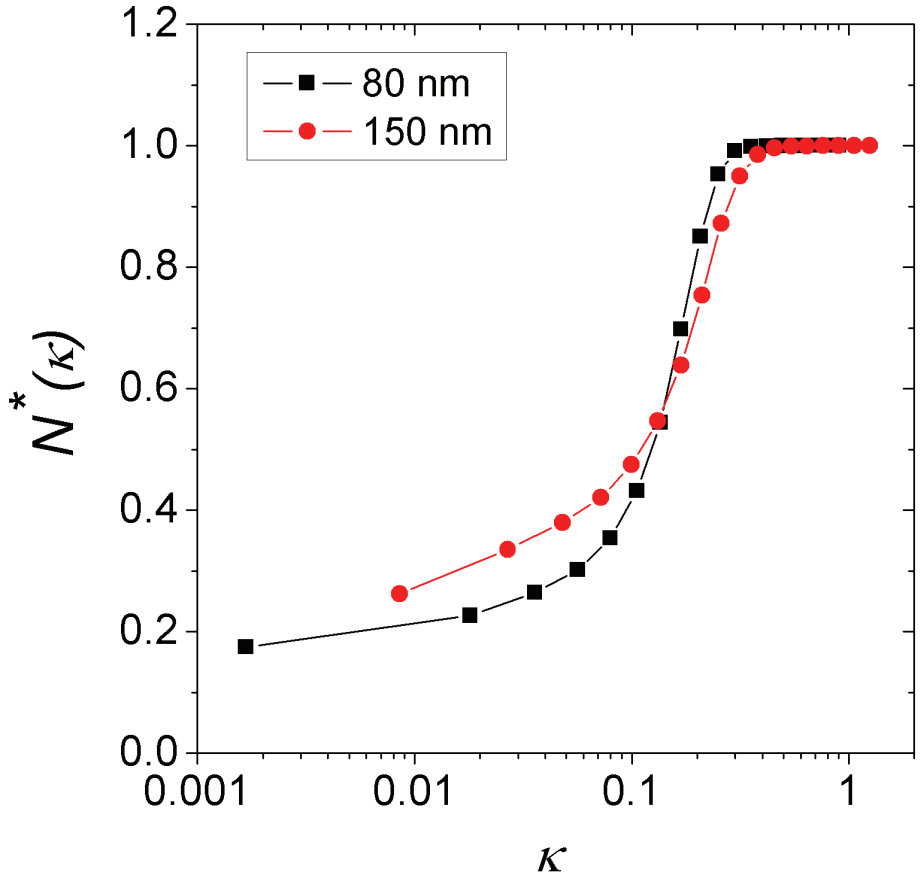

Fig. 1. Normalized cumulative particle hygroscopicity distributions $N^*(\kappa)$ calculated from exemplary HTDMA measurements performed in Beijing (one-day average for 12 June 2004). The dry particle diameters selected by the first DMA were 80 nm and 150 nm, further details can be found in the work of Massling et al. (2009).

ACPD
10, 1005–1034, 2010

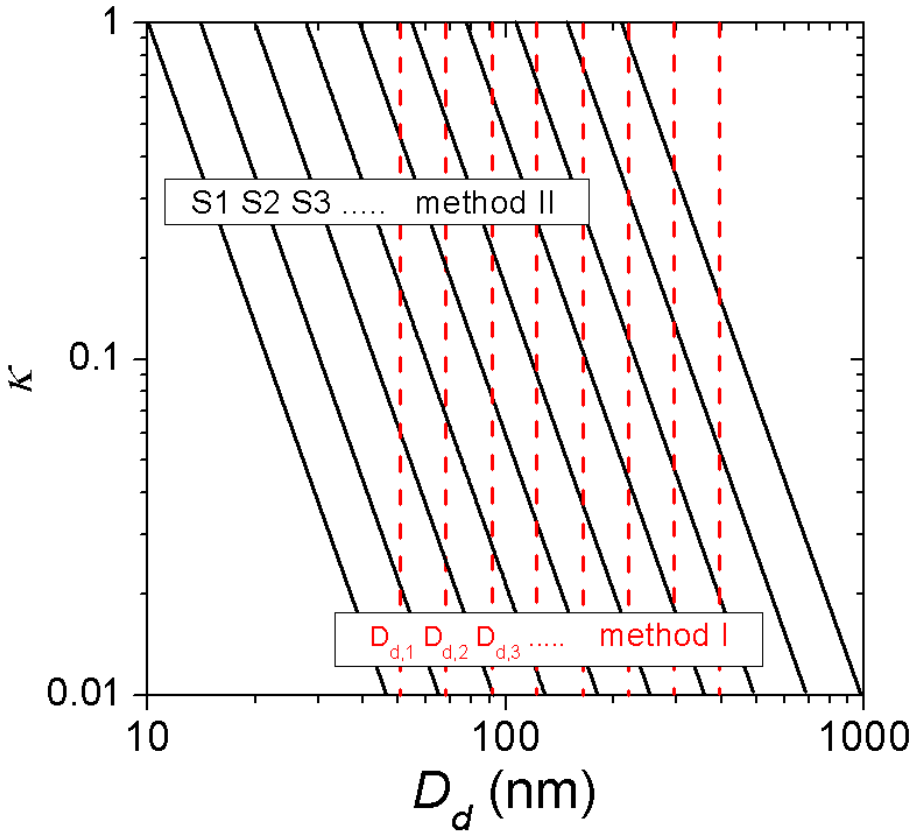

Fig. 2. Two methods of probing particle hygroscopicity (κ) by CCN measurements: (1) method I or "S scan" is represented by vertical dashed lines, in which the dry particle diameter D_d is first kept constant and the water vapor supersaturation S is varied, then choosing another D_d and doing the same procedure; (2) method II or "D_d scan" is represented by the tilted solid lines, in which S is first kept constant and D_d is varied, then choosing another S and doing the same procedure.

ACPD
10, 1005–1034, 2010

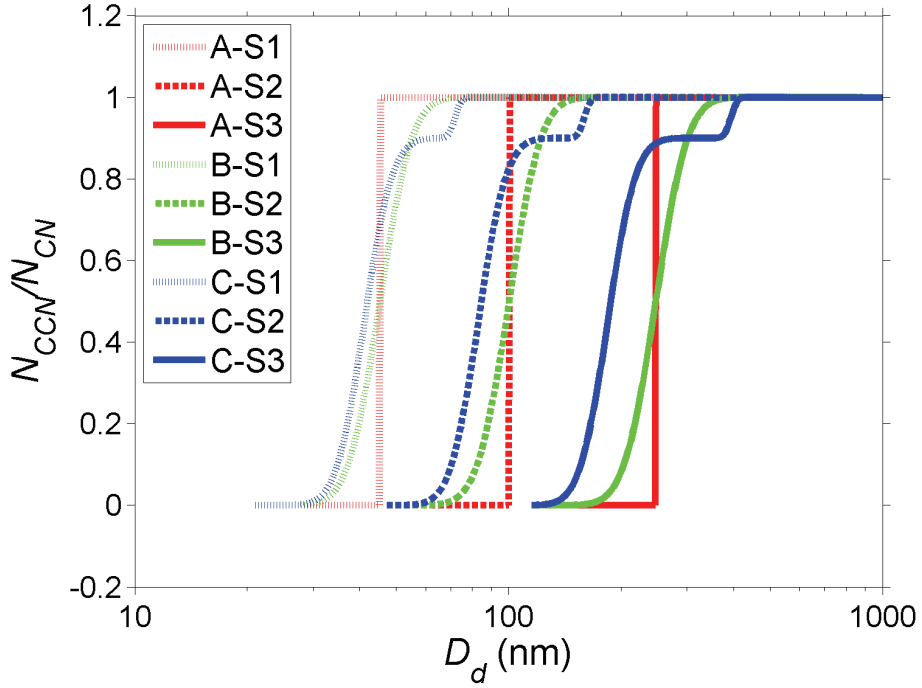

Fig. 3. CCN efficiency spectra of idealized case study aerosols. Each line represents the spectrum of one type of aerosol (Case A, B, or C as specified in Table 1 and Figs. 4–5) measured at a fixed supersaturation S ($S1$=0.86%, $S2$=0.26%, or $S3$=0.067%).

ACPD
10, 1005–1034, 2010

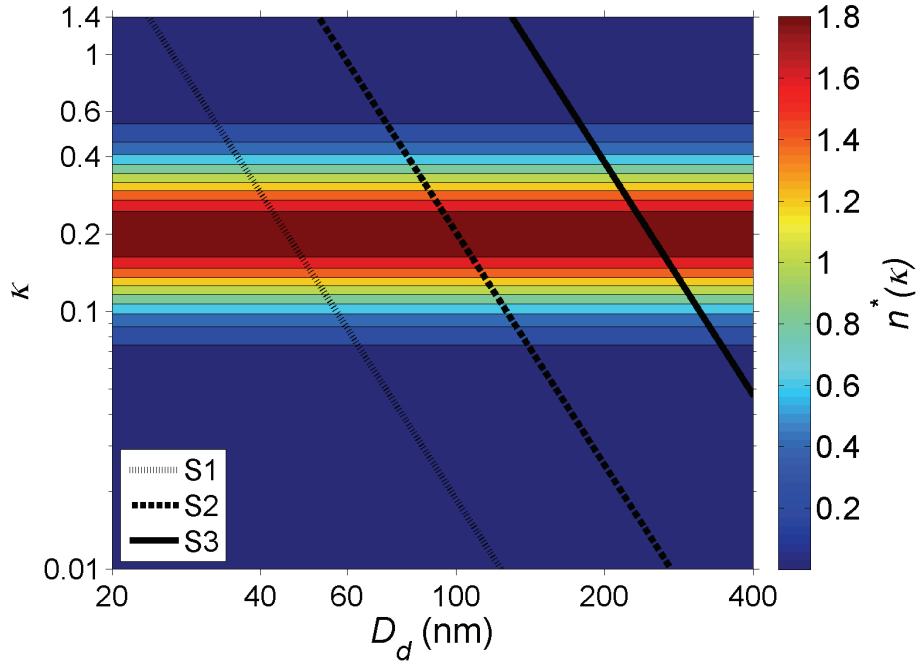

Fig. 4. Normalized particle hygroscopicity distribution, $n^*(\kappa)$, plotted over effective hygroscopicity parameter (κ) and dry particle diameter (D_d) for Case B.

ACPD
10, 1005–1034, 2010

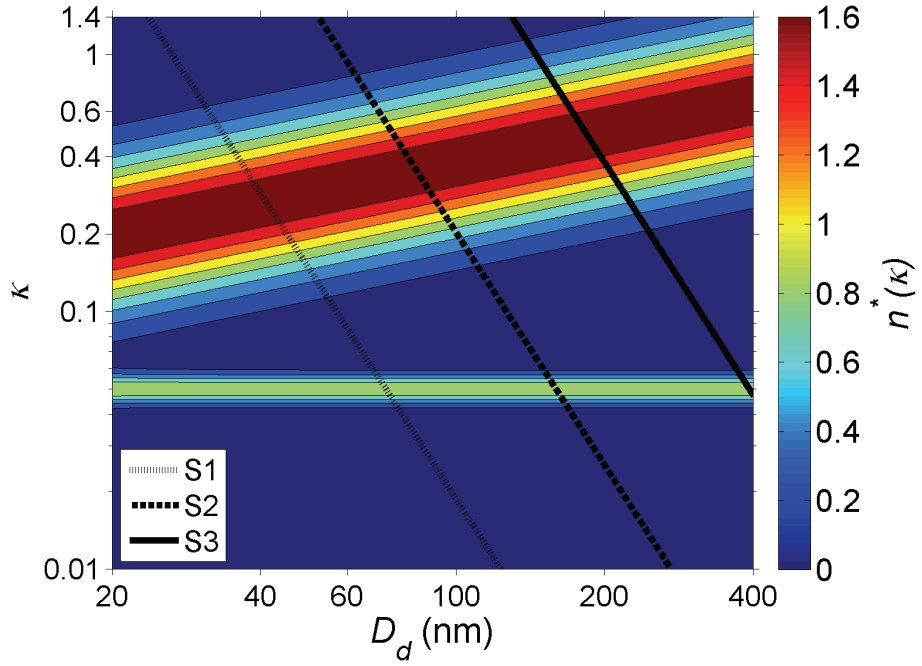

Fig. 5. Normalized particle hygroscopicity distribution, $n^*(\kappa)$, plotted over effective hygroscopicity parameter (κ) and dry particle diameter (D_d) for Case C.

ACPD
10, 1005–1034, 2010

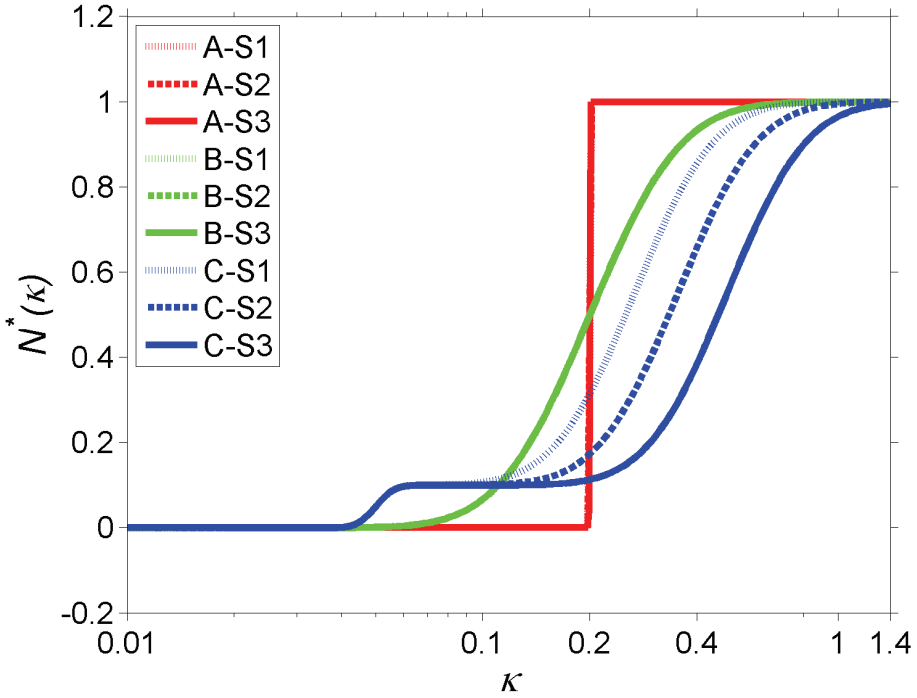

Fig. 6. Normalized cumulative particle hygroscopicity distribution, $N^*(\kappa)$, calculated from the CCN efficiency spectra of idealized case study aerosols (Fig. 3). Each line represents the cumulative distribution of one type of aerosol (Case A, B, or C, as specified in Table 1 and Figs. 4–5) at a fixed supersaturation S ($S1$=0.86%, $S2$=0.26%, or $S3$=0.067%).

ACPD
10, 1005–1034, 2010

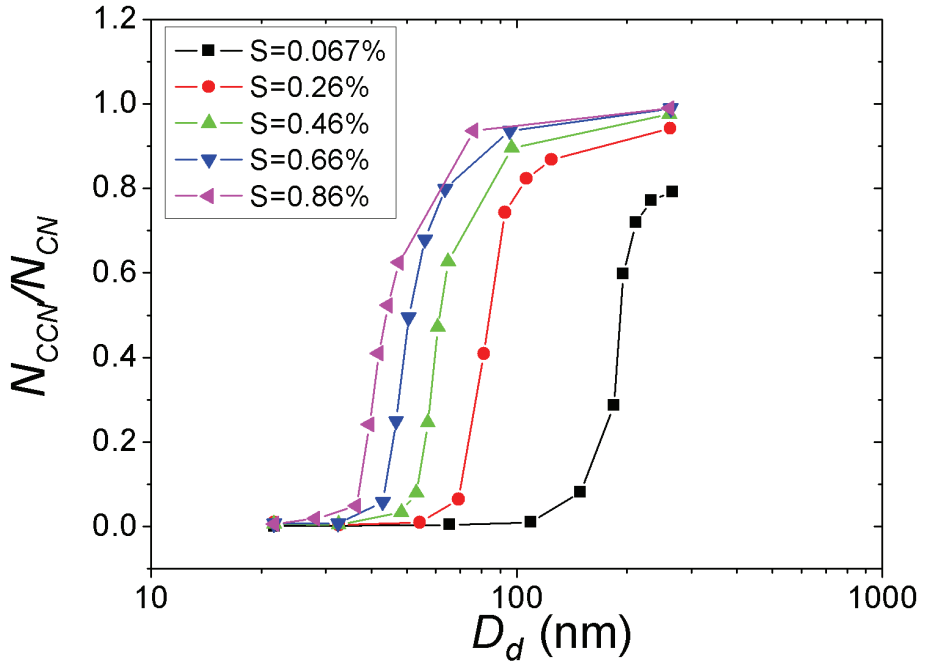

Fig. 7. CCN efficiency spectra of polluted megacity air in Beijing (CAREBEIJING 2006 campaign average).

ACPD
10, 1005–1034, 2010

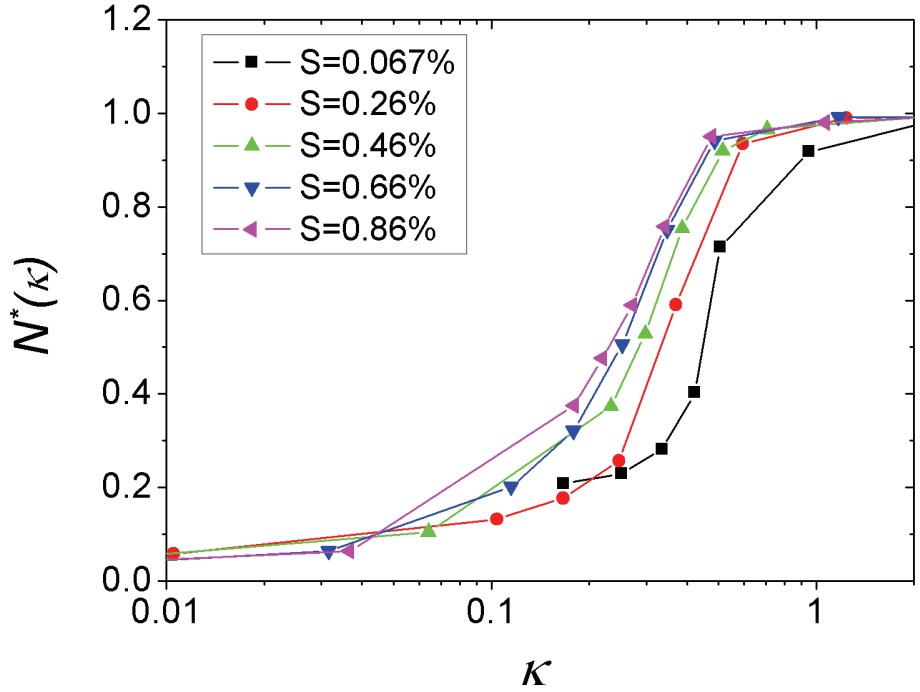

Fig. 8. Normalized cumulative particle hygroscopicity distribution, $N^*(\kappa)$, corresponding to the CCN efficiency spectra observed in Beijing (Fig. 7).

ACPD
10, 1005–1034, 2010

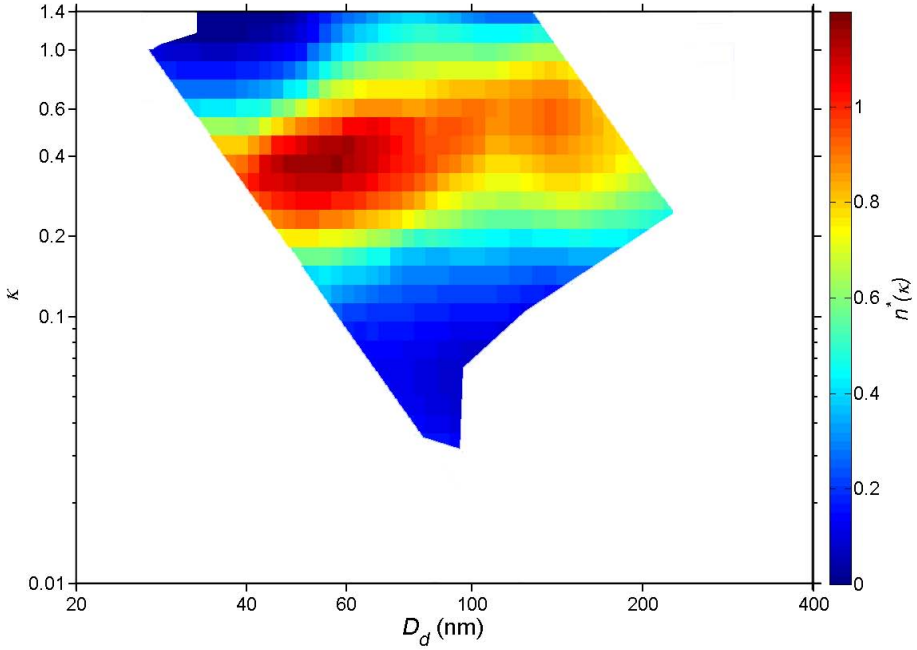

Fig. 9. Normalized particle hygroscopicity distribution, $n^*(\kappa)$, calculated from the cumulative distributions $N^*(\kappa)$ of Fig. 8. Measurement-derived values of $n^*(\kappa)$ were interpolated with a "loess" smooth method (local regression using weighted linear least squares and a 2nd degree polynomial model).

ACPD
10, 1005–1034, 2010